

AGASA Results (Anisotropy)

Masahiro TAKEDA and THE AGASA COLLABORATION *

Institute for Cosmic Ray Research, University of Tokyo, Chiba 277-8582, Japan

(Received October 19, 2001)

Small-scale anisotropy of extremely high energy cosmic rays observed with the Akeno Giant Air Shower Array (AGASA) is studied. Above 4×10^{19} eV, one triplet and five doublets were observed within the angular separation of 2.5° . The self-correlation separation angle distribution shows a sharp peak in the narrow scale of 2.5° with a statistical significance of 4.6σ . This distribution is consistent with the angular resolution of the AGASA detector. Even in the lower energy range above 10^{19} eV, we also found a relatively weak correlation with angular spread within 4° . These experimental results indicate compact sources for the extremely high energy cosmic ray clusters. Another interesting feature of clusters is that the events contributing to clusters would have a hard energy spectrum.

§1. Introduction

Recent observations of extremely high energy cosmic rays have shown the extension of the cosmic-ray energy spectrum beyond 10^{20} eV,^{1,2)} and enhanced an interest of their origin for the following reasons: Firstly, any traditional mechanism could hardly have a reasonable capability of accelerating cosmic ray particles up to energies above 10^{20} eV. Secondly, a cutoff of the cosmic-ray energy spectrum has been expected at around 4×10^{19} eV due to the Greisen-Zatsepin-Kuz'min (GZK) effect^{3,4)} through resonant hadron production when such high energy cosmic rays interact with the cosmic microwave background radiation. The GZK effect limits the propagation length of cosmic rays above 10^{20} eV to within 50 Mpc from our Galaxy,⁵⁻⁷⁾ while no astronomical counterpart with enough acceleration capability has been found within this distance. Accumulated experimental data shows increasing inconsistency with conventional models for the origin of cosmic rays based on acceleration by astronomical objects.

Study of the arrival direction distribution plays a key role in solving the origin of the highest energy cosmic rays. There have been many studies of large-scale anisotropy,⁸⁻¹²⁾ however large-scale anisotropy has not been established in the highest energy range due to limited statistics. Recently, small-scale anisotropy – clusters of events in arrival direction distribution – was reported by several authors.^{9,13-16)} With the increase of experimental data, mainly from the AGASA experiment, more sophisticated analysis is now possible: A cross-correlation study with astronomical objects¹⁷⁾ and a self-correlation study.¹⁸⁾ In this paper, we examine small-scale anisotropy of extremely high energy cosmic rays using updated AGASA data up to the end of 2000.

Table I. Number of events in the data set.

Array	$\geq 10^{19}$ eV	$\geq 4 \times 10^{19}$ eV	$\geq 10^{20}$ eV
A20	59	7	0
AGASA	716	52	8
Total	775	59	8

§2. Experiment

The Akeno Observatory is situated at $138^\circ 30'$ E and $35^\circ 47'$ N. AGASA consists of 111 surface detectors deployed over an area of about 100 km^2 , and has been in operation since 1990.^{19,20)} A prototype system called A20 had been operated in Akeno from 1984 to 1990,²¹⁾ and became an integral part of AGASA since 1990. The details of the AGASA instrumentation have been described in the above references.¹⁹⁻²¹⁾ In this analysis, we have selected events with zenith angles smaller than 45° and with core locations inside the array area. The number of events until the end of 2000 are listed in Table I. Above 4×10^{19} eV, two more doublets were detected in the updated data set. The number of clusters appears to increase steadily with AGASA exposure.

The accuracy on determination of shower parameters were evaluated through the analysis of a large number of artificial events. These artificial events were generated by taking account for air shower features and fluctuation determined experimentally. Figure 1 shows the accuracy on arrival direction determination for cosmic-ray induced air showers as a function of energies. The vertical axis denotes the opening angle $\Delta\theta$ between input (simulated) and output (analyzed) arrival directions. The opening angles including 68 % and 90 % of data are plotted. By analyzing artificial events with the same algorithm used above, the accuracy on energy determination is estimated to be $\pm 30 \%$ above 10^{19} eV.

* <http://www-akeno.icrr.u-tokyo.ac.jp/AGASA/>

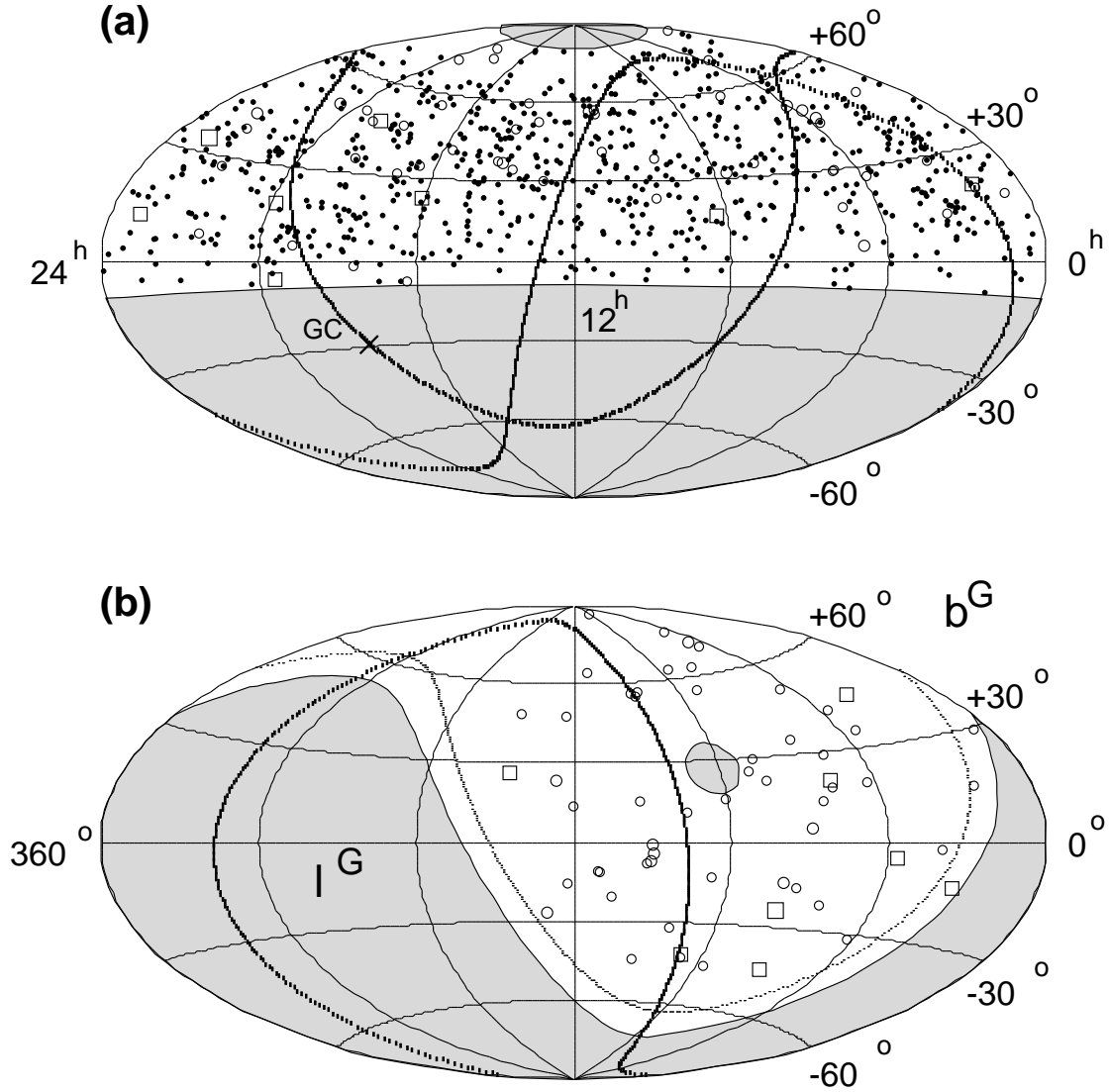


Fig. 2. Arrival directions of cosmic rays with energies above 10^{19} eV in (a) Equatorial and (b) Galactic coordinates. Dots, circles, and squares represent cosmic rays with energies of $(1-4) \times 10^{19}$ eV, $(4-10) \times 10^{19}$ eV, and $\geq 10^{20}$ eV, respectively. The shaded regions indicate the celestial regions excluded in this paper due to the zenith angle cutoff of $\leq 45^\circ$. “GC” designates the Galactic center.

§3. Results

Figure 2(a) shows arrival directions of cosmic rays with energies above 10^{19} eV in equatorial coordinates. Dots, circles, and squares represent cosmic rays with energies of $(1-4) \times 10^{19}$ eV, $(4-10) \times 10^{19}$ eV, and $\geq 10^{20}$ eV, respectively. Figure 2(b) shows arrival directions of cosmic rays only above 4×10^{19} eV in Galactic coordinates. Clusters of cosmic rays within small separation angles can be seen in this figure. Details of cosmic rays above 4×10^{19} eV are available on our web page.²²⁾

3.1 Cluster Analysis

First of all, we follow the same procedure of the cluster analysis described in §3.4 of our ApJ paper.¹⁵⁾ A cluster of cosmic rays is defined as follows:

1. Define the i -th event;
2. Count the number of events within a circle of radius 2.5° centered on the arrival direction of the i -th event;
3. If this number of events exceeds a certain threshold value N_{th} , the i -th event is counted as a cluster.

This sequence was repeated for all 59 events above 4×10^{19} eV, and the total number of clusters for N_{th} was determined. The chance probability P_{ch} of observing this number of clusters under an isotropic distribution is obtained from the distribution of the number of clusters using 10,000 simulated data sets. These simulated data sets were also analyzed by the same sequence described above. Out of 10,000 simulations, 5 trials had the same amount of or more doublets ($N_{th} = 2$) than the observed

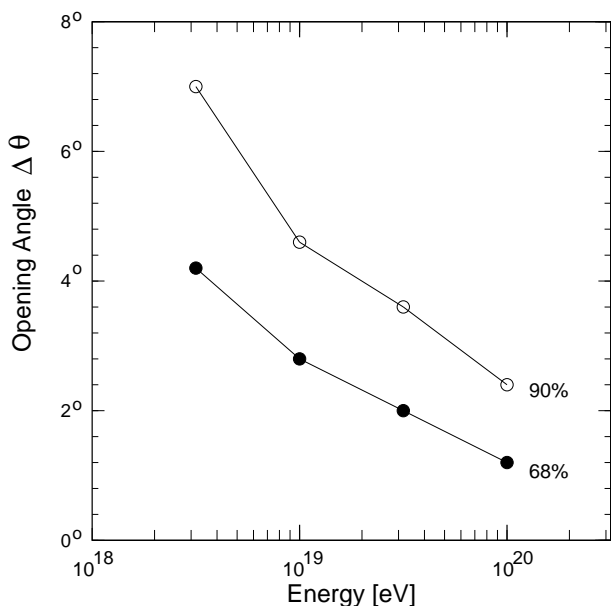


Fig. 1. Accuracy on arrival direction determination. Closed and open circles are the opening angles encompassing 68 % and 90 % data, respectively.

data set, so that $P_{ch} = 0.05\%$; $P_{ch} = 1.66\%$ for triplets ($N_{th} = 3$).

Here, simulated data sets have a uniform distribution in right ascension and declination and energy distributions which follow experimental observations of AGASA. The uniformity of the observation time in right ascension results from the uniform observation in solar time over more than ten years. This is expected for a surface array detection system such as AGASA operating in stable conditions. The fluctuation of the observation time in local sidereal time is only $(0.2 \pm 0.1)\%$, which is small enough compared with the anisotropy in the energy range of interest, such that the exposure in right ascension is quite uniform. The declination distribution reflects the zenith angle dependence of the AGASA exposure and is consistent with the distribution expected if cosmic rays come isotropically from the celestial sphere. Since the trigger efficiency is independent of energy above 10^{19} eV at a zenith angle less than 45° , this distribution is applicable to higher energies.

Next, the energy dependence for observing doublets and triplets are estimated, and the results are shown in Figure 3. When a new cluster is added above a threshold energy, a histogram changes discontinuously at that energy. At the maximum threshold energy where the triplet is detected, we find $P_{ch} = 0.19\%$ in Figure 3(b). The narrow peaks above 4×10^{19} eV in Figure 3(a) result from the C1, C2 (triplet), ..., C7 clusters; C5 is found just below 4×10^{19} eV (see Table II). The chance probabilities in this figure are estimated without taking account for the degree of freedom on the threshold en-

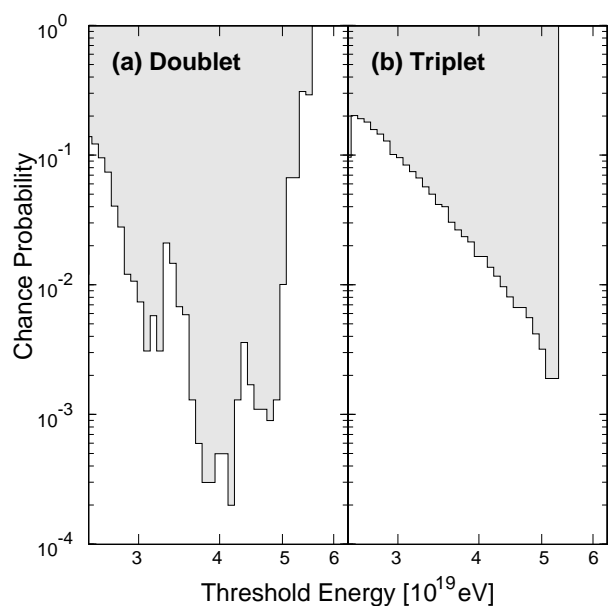


Fig. 3. Energy dependence of the chance probability of observing (a) doublets and (b) triplets.

ergy. However, the chance probabilities are smaller than 0.1 % for doublets and 1 % for triplets in this range. The smallest chance probabilities are obtained around 4×10^{19} eV, and this energy may indicate some critical energy for clusters.

Table II. AGASA Clusters above 4×10^{19} eV.

	Energy ($\times 10^{19}$ eV)	Time (MJD)	α	δ
C1	21.3	49324.52	$1^h 15^m$	21.1°
	5.07	50018.65	$1^h 14^m$	20.0°
C2	5.50	48835.17	$11^h 29^m$	57.1°
	7.76	49742.77	$11^h 14^m$	57.6°
C3	5.35	50907.46	$11^h 13^m$	56.0°
	4.35	48365.98	$18^h 59^m$	47.8°
C4	13.4	49539.48	$18^h 47^m$	48.5°
	5.47	46435.44	$4^h 38^m$	30.1°
C6	4.89	50035.81	$4^h 41^m$	29.9°
	4.97	50440.94	$14^h 17^m$	37.7°
C7	4.98	51690.40	$14^h 08^m$	37.1°
	6.11	51112.66	$3^h 45^m$	44.9°
C5	4.20	51813.78	$3^h 41^m$	46.6°
	14.4	50093.00	$16^h 06^m$	23.0°
	(3.89)*	50547.74	$15^h 58^m$	23.7°

* This event is just below the threshold energy of 4×10^{19} eV.

To check the clustered events above 4×10^{19} eV didn't arise from the system instability, the Kolmogorov-Smilnov (KS) test for the event distribution on the horizontal coordinates and time was carried out. The results are summarized in Table III, and these KS probabilities are large enough to consider that clustered events uniformly distribute on the horizontal coordinates and time.

Table III. KS test for the clustered events distribution on the horizontal coordinates and time.

	KS Probability
Observed time	0.986
Azimuth angle	0.209
Zenith angle	0.802
Right ascension	0.285
Declination	0.152
Galactic longitude	0.407
Galactic latitude	0.597
Supergalactic longitude	0.281
Supergalactic latitude	0.291
Ecliptic longitude	0.559
Ecliptic latitude	0.365

3.2 Self-Correlation Analysis

In the above cluster analysis, certain conditions of $(\theta, N_{th}) = (2.5^\circ, 2)$ and $(2.5^\circ, 3)$ are demonstrated. Any possible conditions were also examined with a step of 0.5° for θ and 1 for N_{th} , and the original condition of $(2.5^\circ, 2)$ was found to be most significant. To show clear dependence on the separation angle θ , self-correlation analysis, which was introduced by Tinyakov and Tkachev,¹⁸⁾ is applied.

Figure 4 shows the result of the self-correlation analysis. The vertical axis indicates an event density:

$$N(\theta) = \sum_i \sum_{j \neq i} R_{ij}(\theta) / S(\theta), \quad (3.1)$$

where

$$R_{ij}(\theta) = \begin{cases} 1 & \text{if } \theta_{ij} \text{ in } d\theta \\ 0 & \text{otherwise} \end{cases},$$

and θ_{ij} is the separation angle of two events on the celestial sphere and $S(\theta)$ is the area of a concentric ring at $\theta d\theta$. This density increases as multiplicity of clusters increases. The histogram is the observed distribution and the solid curve is that expected under an isotropic distribution. There is a clear sharp peak at small separation angles. No statistically significant deviation from the expected curve was observed at larger separation angles. This peak results from the six clusters: one triplet and five doublets listed in Table II, and two of the five have been obtained since writing the previous paper.¹⁵⁾ The separation angles are smaller than 2.5° , which is comparable to $\sqrt{2} \times \Delta\theta_{68\%}(E = 4 \times 10^{19} \text{eV})$ in this energy range and corresponds to the AGASA angular resolution. The point spread function of AGASA (dashed curve in Figure 4(a)) is obtained from Monte-Carlo simulations to derive the accuracy of determination of shower parameters. This PSF curve fits well to the observed distribution. This means that the clusters are regarded as point-like sources given the AGASA angular resolution. From 10,000 simulated data sets, the average and deviation of the number of clusters, within $r(E) = \sqrt{2} \times \Delta\theta_{68\%}(E)$ at $E = 4 \times 10^{19} \text{eV}$, is derived to be 1.7 and 1.36, respectively. The observed number of pairs is $(5 + 1 \times 3)$, and

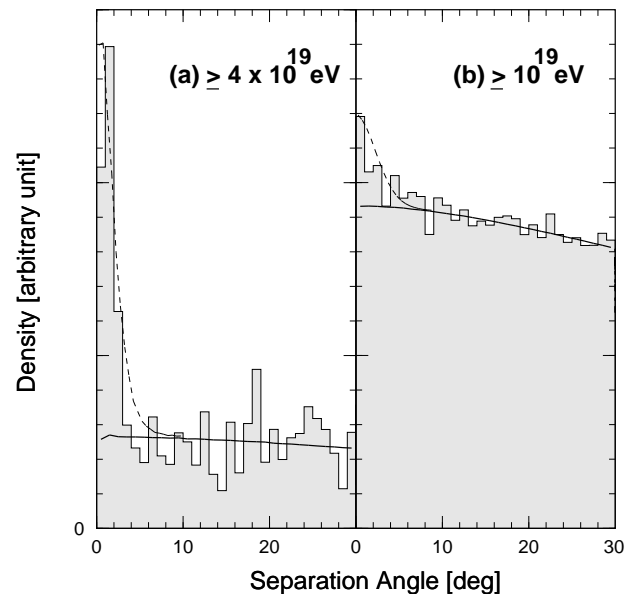


Fig. 4. Self-correlation analysis with energies above (a) $4.0 \times 10^{19} \text{eV}$ and (b) $1.0 \times 10^{19} \text{eV}$. (Histogram: observed data set; Curve: average of 10,000 simulated data sets; Dashed curve: the AGASA point spread function)

then the significance of this peak is 4.6σ .

Another threshold energy of 10^{19}eV is the bending energy “ankle” of the cosmic-ray energy spectrum. Above this energy, arrival directions are shown in Figure 2(a). Here, some clusters of 10^{19}eV events which were appeared in our previous paper¹⁵⁾ are shown again. Figure 4(b) shows the self-correlation analysis for cosmic rays above 10^{19}eV , and a small peak is observed. The separation angle of this peak is less than 4° , and this is in good agreement with the AGASA point spread function represented by the dashed curve. The significance of deviation from the expected distribution is $(675 - 613.6) / 26.9 = 2.3\sigma$. While the significance of this peak is small, it is worth noting that these peaks in the self-correlation analysis observed with energies above $4 \times 10^{19} \text{eV}$ and 10^{19}eV are consistent with the AGASA point spread functions.

Here, the threshold energy dependence in the self-correlation analysis is estimated. Figure 5 shows the number of clusters both in the observed (histogram) and simulated (curve) data sets using the energy-dependent separation angles $r(E)$ (see Figure 1). The simulated data sets were obtained from 10,000 trials under an isotropic distribution, and their average N_{exp} and deviation ΔN_{exp} were derived. Figure 6 shows the statistical significance of excess of the number of clusters. Within the energy resolution of AGASA, the significance of excess around $4.5 \times 10^{19} \text{eV}$ are obtained to be above about 4σ , while excess for the lower threshold energies are not so significant.

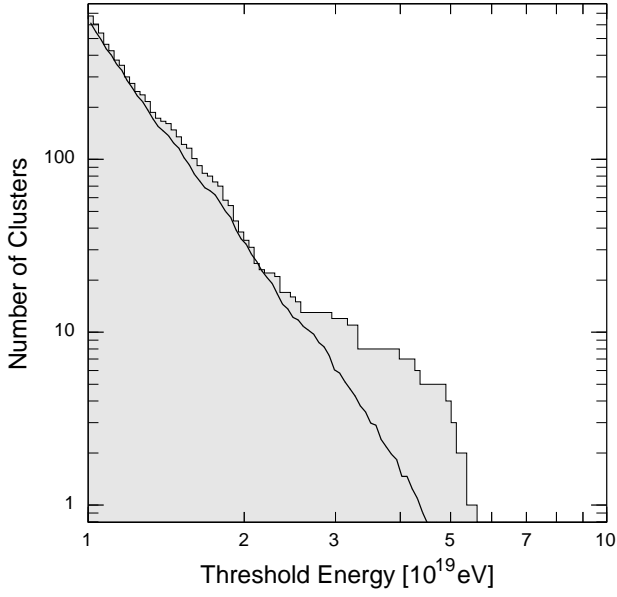


Fig. 5. Number of clusters in the self-correlation analysis. The energy dependence on the separation angle $r(E)$ is used.

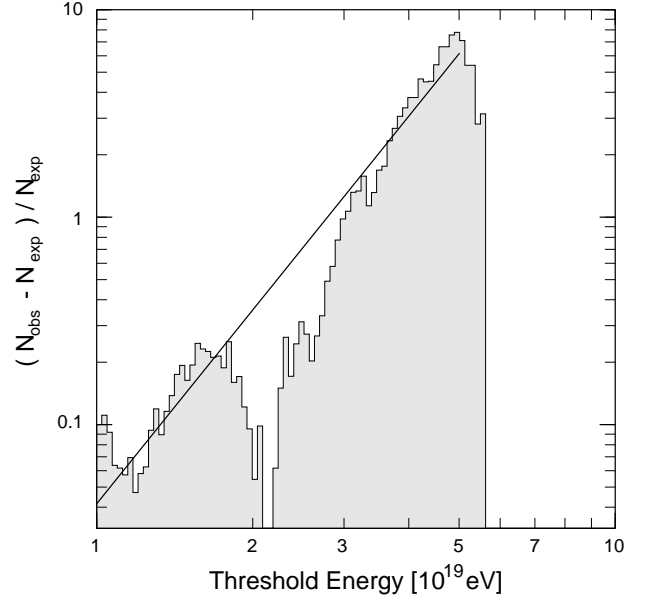


Fig. 7. $(N_{obs} - N_{exp})/N_{exp}$ in the self-correlation analysis. The values N_{obs} , N_{exp} are same in Figure 5.

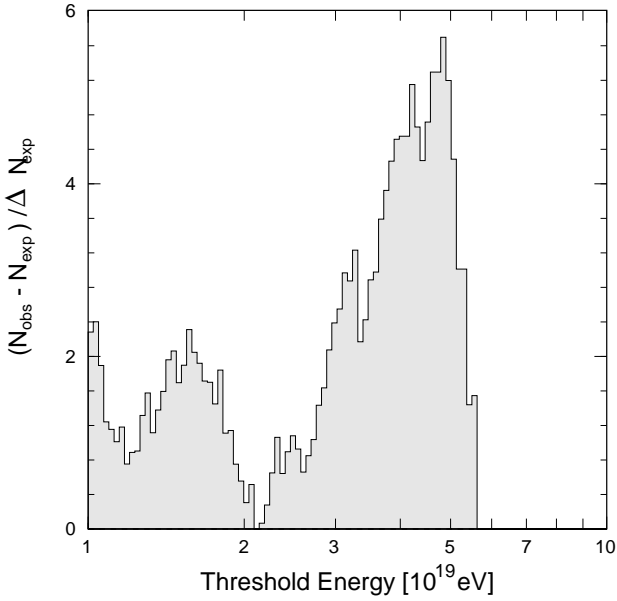


Fig. 6. $(N_{obs} - N_{exp})/\Delta N_{exp}$ in the self-correlation analysis. The values N_{obs} , N_{exp} are same in Figure 5.

Figure 7 shows the ratio of $(N_{obs} - N_{exp})/N_{exp}$. The clear relation can be seen and it is expressed by

$$\frac{N_{obs} - N_{exp}}{N_{exp}}(\geq E) \propto E^{3.10 \pm 0.10}, \quad (3.2)$$

where the energy range is $(1 - 5) \times 10^{19}$ eV. This may indicate an interesting feature of clusters. The ratio of clus-

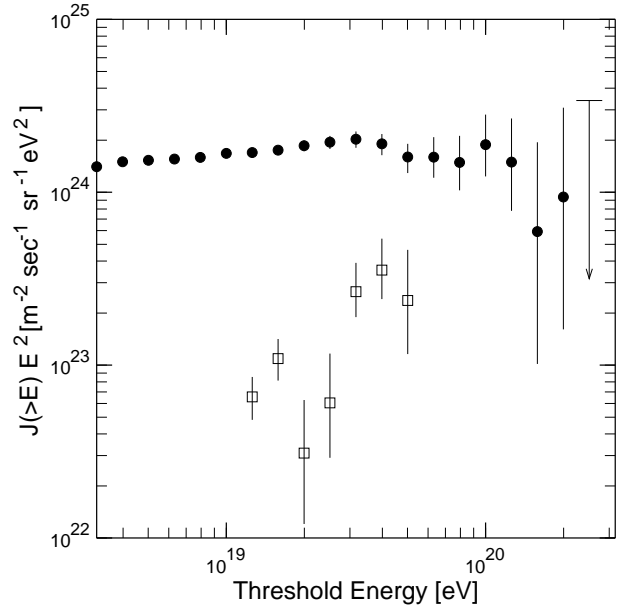


Fig. 8. Integral energy spectrum of cosmic rays contributing clusters (open squares) with the AGASA integral spectrum (closed circles).

ter “signal” components, which are the excess of events contributing to clusters with the angular size of $r(E)$, increases with energy and is estimated to be 10^{-3} , 5×10^{-2} , and 10^{-1} of the integral cosmic-ray flux observed with AGASA in energies above 10^{19} eV, 2×10^{19} eV, and 4×10^{19} eV, respectively. Figure 8 shows this situation; Open squares are the integral energy spectrum of the

cluster “signal” components, and closed circles indicate the AGASA integral energy spectrum. The integral energy spectrum of the cluster “signal” components is not a source spectrum but the observed spectrum. There are large fluctuations on the number of pair event components, however, its ratio to all particles grows rapidly as a function of energy up to 3×10^{19} eV. At higher energy part, this ratio looks to be constant. If we correct the counting efficiency taking into account the number of “singlets” from clusters (they are not recognized as a member of pair due to poor statistics), the real intensity from clusters will increase especially at higher energy part. As a whole, the integral energy spectrum of the “signal” components is hard although the error bars are very large, and its integral spectral index is $-0.8 \pm 0.7(\text{stat}) \pm 0.4(\text{sys})$ corresponding to the differential index of -1.8 if we dare to evaluate it. The large error in the evaluated spectral index arises from a deficit around 2×10^{19} eV. This deficit would occur from statistical fluctuation, however it looks strange. So, we are in progress on this feature.

3.3 How many sources

Next, we estimate the number of sources if we assume all observed events above 4×10^{19} eV came from a particular type of source. Sources have the following conditions:

1. The number of sources is N_S ;
2. The frequency of observation of cosmic rays from each of sources follows the Poisson distribution $P(x, \mu)$ with an average μ : $x = 3$ (2) corresponding to sources of a triplet (doublet) and $x = 0$ is a non-observed source.

From multiplicity distribution of $N_x = 46, 5, 1, 0, 0$ at $x = 1, 2, \dots, 5$, we obtained the reduced χ^2 distribution (histogram) and N_S (curve) against μ as shown in Figure 9, and found $N_S \simeq 220_{-100}^{+207}$ for $\mu = 0.27_{+0.30}^{-0.14}$ with 68 % C.L. Here, we neglected characteristics and distances of sources, and it is important to note that we don't know how many fraction of $N_{x=1}$ results from the assumed type of source. If we consider two (or more) types of source, one of which corresponds to a “cluster” component with a hard spectrum, $N_S \simeq 427$ is the upper limit for the number of sources in the observed celestial region. However, the other experiments – such as the Volcano Ranch, Haverah Park and Yakutsk experiments – show only weak correlation with the AGASA clusters (see Uchihori et al.¹⁶⁾), and this is possibly consistent with the number of sources above 4×10^{19} eV being a few hundreds.

§4. Discussion

The physical implication of this work is in favor of neutral particles as a primary of clustered events. The clusters' positions are statistically isotropic on the celestial sphere and there is no correlation or anti-correlation with the Galactic plane or the structure of the Galactic magnetic field. Protons with $p = 10^{19}$ eV/c bend their trajectories by several degrees in arrival directions, espe-

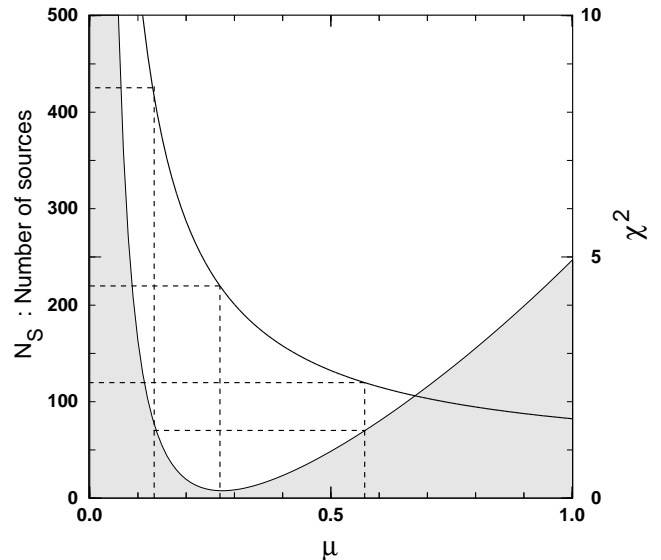


Fig. 9. Number of sources expected from the multiplicity of clusters. The dotted lines indicate the χ^2 minimum and upper and lower bound with 68 % C.L.

cially $\sim 10^\circ$ near the Galactic plane. However, we cannot see such a signature in our data set. We have also examined time correlation of clustered events. We found no significant time correlation within a few years time scale among the events contributing to clusters above 4×10^{19} eV.

In conclusion, a fraction of extremely high energy cosmic rays above 4×10^{19} eV are clustered: one triplet and five doublets were observed in this energy range. The separation angle distribution, above 4×10^{19} eV and 10^{19} eV, in a self-correlation analysis show peaks with 4.6 σ and 2.3 σ significance, respectively, and they follow the point spread function of the AGASA experiment taking account of the angular resolution. The cosmic rays contributing to clusters are expected to have a hard energy spectrum. The multiplicity of clusters above 4×10^{19} eV tells that the upper limit for the number of their sources is expected to be $\simeq 427$ in the observed celestial region. However, it is still open as to whether or not source density varies over various celestial regions. To reveal this, much better statistics, expected from the next generation experiments, is required.

Acknowledgements

We are grateful to Akeno-mura, Nirasaki-shi, Sudama-cho, Nagasaka-cho, Ohizumi-mura, and the Tokyo Electric Power Co., and Nihon Telegram and Telephone Co. for their kind cooperation. The authors are indebted to other members of the Akeno group for the maintenance of the AGASA array. This work is supported in part by JSPS grants in aid of the scientific research #12304012 and #11691117. M.Takeda gratefully acknowledges receipt of a JSPS Research Fellowship.

-
- 1) M. Takeda *et al.*, Phys. Rev. Lett., **81** (1998), 1163.
 - 2) D. J. Bird *et al.*, Ap. J. **441** (1998), 144;
 - 3) K. Greisen, Phys. Rev. Lett. **16** (1966), 748.
 - 4) G. T. Zatsepin and V. A. Kuz'min, Zh. Eksp. Teor. Fiz. **4** (1966), 114 [JETP Letters **4** (1966) 78].
 - 5) C. T. Hill and D. N. Schramm, Phys. Rev. **D 31** (1984), 564.
 - 6) V. Berezhinsky and S. I. Grigor'eva, Astron. Astrophys., **199** (1988), 1.
 - 7) S. Yoshida and M. Teshima, Prog. Teor. Phys., **89** (1993), 833.
 - 8) M. S. Gillman, and A. A. Watson, in *Proceedings of the 23th International Cosmic Ray Conference, Calgary, 1993* (University of Calgary, Calgary, 1993) Vol. 2, p. 47.
 - 9) N. Hayashida *et al.*, Phys. Rev. Lett., **77** (1996), 1000.
 - 10) L. J. Kewley, R. W. Clay, and B. R. Dawson, Astropart. Phys., **5** (1996), 69.
 - 11) N. Hayashida *et al.*, Astropart. Phys., **10** (1999), 303.
 - 12) D. J. Bird *et al.*, Ap. J., **511** (1999), 739.
 - 13) X. Chi *et al.*, in "Astrophysical Aspects of the Most Energetic Cosmic Rays", ed. M. Nagano and F. Takahara (Singapore: World Scientific, 1991), p. 140.
 - 14) T. Stanev *et al.*, Phys. Rev. Lett., **75** (1995), 3056.
 - 15) M. Takeda *et al.*, Ap. J., **522** (1999), 225 [astro-ph/9902239].
 - 16) Y. Uchihori *et al.*, Astropart. Phys., **13** (2000), 151.
 - 17) G. R. Farrar & P. L. Biermann, Phys. Rev. Lett., **81** (1998), 3579; Phys. Rev. Lett., **83** (1999), 2478.
 - 18) P. G. Tinyakov and I. I. Tkachev, to be published in Phys. Rev. Lett., [astro-ph/0102101].
 - 19) N. Chiba *et al.*, Nucl. Instr. Meth., **A 311** (1992), 338.
 - 20) H. Ohoka *et al.*, Nucl. Instr. Meth., **A 385** (1997), 268.
 - 21) M. Teshima *et al.*, Nucl. Instr. Meth., **A 247** (1986), 399.
 - 22) <http://www-akeno.icrr.u-tokyo.ac.jp/AGASA/pub/>